Journal of
Marine Science and Engineering

MDPI

Article

Tailoring the Fatigue Detail Category Class: A Deterministic Implementation of a Probabilistic-Based Approach to Consequence- and Uncertainty-Informed Fatigue Life Prediction of Ships †

Marije L. Deul *, Coen H. H. van Battum and Martijn Hoogeland

Netherlands Organisation for Applied Scientific Research (TNO), Molengraaffsingel 8, 2629 JD Delft, The Netherlands; coen.vanbattum@tno.nl (C.H.H.v.B.); martijn.hoogeland@tno.nl (M.H.)
* Correspondence: marije.deul@tno.nl

† This paper is an extended version of our paper published in the proceedings of MARSTRUCT 2023 conference and proceedings.

Abstract: The fatigue life of ship structures is typically based on deterministic methods in which underlying uncertainties are only implicitly taken into account and not explicitly reflected. Guidance for a probabilistic assessment is provided in class documents, but the methodology is too time consuming to apply in design practice. This paper proposes a novel approach based on DNV-CG-0129 to incorporate uncertainties and consequences explicitly. Using a probabilistic model, tailored deterministic FAT classes are derived to be applied in design practice. A tailored FAT class should be selected based on an acceptable probability of failure related to the severity of the consequences of a failure for the ship. Results show that tailored FAT classes are strongly dependent on the uncertainties provided as input when using the calculation method of DNV-CG-0129. This emphasizes the need for careful consideration and specification of the uncertainties. Furthermore, application of the First Order Reliability Method for a sensitivity study shows that the global model uncertainty is governing over other uncertainties considered in DNV-CG-0129. The proposed approach enables a low-effort and transparent probabilistic-based method, leading to optimized and improved designs due to reduction of overdimensioning in non-critical areas.

Keywords: fatigue reliability; fatigue design; uncertainty; welded joints; probabilistic fatigue; S–N curve; FAT class; Design Fatigue Factor; risk matrix

check for updates

Citation: Deul, M.L.; van Battum, C.H.H.; Hoogeland, M. Tailoring the Fatigue Detail Category Class: A Deterministic Implementation of a Probabilistic-Based Approach to Consequence- and Uncertainty -Informed Fatigue Life Prediction of Ships. *J. Mar. Sci. Eng.* **2023**, *11*, 1715. https://doi.org/10.3390/jmse11091715

Academic Editors: Jonas W. Ringsberg and Carlos Guedes Soares

Received: 10 August 2023
Revised: 22 August 2023
Accepted: 23 August 2023
Published: 31 August 2023

Copyright: © 2023 by the authors. Licensee MDPI, Basel, Switzerland. This article is an open access article distributed under the terms and conditions of the Creative Commons Attribution (CC BY) license (https://creativecommons.org/licenses/by/4.0/).

1. Introduction

Deterministic fatigue analyses have been the standard in the design practice of today, while probabilistic based methods have been available for decades. Probabilistic methods may give weight savings and cost reduction by quantifying the uncertainties in the design, construction, and operation phase, especially in combination with a monitoring system. However, the application of probabilistic methods might increase the analysis time and complexity of the fatigue analysis. This paper is an extended version of our paper published in the proceeding of MARSTRUCT 2023 [1]. Deterministic methods by class societies and guidelines [2–7] are formulated to enable a sufficiently reliable structural design. An often-applied guideline for the fatigue assessment of ship structures is DNV-CG-0129 [5]. Amongst the many parameters to be determined, this class guideline prescribes a conservative lower bound of the S–N curves to account for uncertainties in the fatigue capacity calculation. Deterministic values are used for the Stress Concentration Factor (SCF), cumulative damage used in Miner's rule, and far-field nominal loads based on an idealized structure. The design margins are therefore implicitly modeled with the selection of the design S–N curve and not influenced by the severity of the consequences of a failure for the ship nor by the extent of knowledge regarding actual uncertainties for the considered loads, structure, and detail. However, for optimization and reliability purposes, the explicit design margins should be known. This means that the full formulation (including the mean and standard deviation) of the S–N curve as well as all uncertainties in the analysis are required. The collection and processing of this information tends to be more complex than the currently applied design methods but are required to serve the novel purposes of optimization and reliability assessment.

Besides the method for the deterministic fatigue life prediction, both DNV-RP-C203 [6] (providing the recommended practice for the fatigue design of offshore steel structures) and DNV-CG-0129 [5] (providing a class guideline for the fatigue assessment of ship structures) suggest a probabilistic fatigue life prediction and give guidelines for the uncertainty factors to be applied. The authors have not heard of the application of these probabilistic methods in ship design practice in discussions with class and design representatives. The suggested probabilistic input from [5,6] is the same. However, distinct differences are present between the offshore and shipping industries that should result in differences in especially the assumed global model uncertainties (the uncertainties related to the translation of the load to nominal stresses) and in the acceptance of certain risk levels. The expected differences with respect to the global model uncertainty are related to differences in, e.g., the building process and expected sailing/operational area. The shipping and offshore industries tend to have different approaches to fatigue; this is reflected by the observation that the class guideline for ship structures, DNV-CG-0129 [5], includes information for a probabilistic approach in its Appendix G, whereas the recommend practice for offshore steel structures, DNV-RP-C203 [6], includes the same in the main text.

DNV-RP-C203 [6] incorporates the Design Fatigue Factor (DFF). This DFF is typically applied in the offshore industry as a safety factor to decrease the acceptable accumulated damage for structural details where inspection and repair are more challenging, taking into account the severity of a potential failure. The DFF is equal to one over the critical damage (η) under the assumption of an ergodic load in combination with the Linear Damage Accumulation Model (LDAM) [8,9]. The recommended DFF for offshore structures can be obtained from, e.g., DNV-RP-C203 [6] and DNV-OS-C101 [10]. Deviations from the DFF can be made in correspondence with the client of the ship. DFFs are currently not applied for ship design. Next to that, the linear scale of the DFF in relation to the fatigue life does not accurately reflect the non-linear nature of the probability density function of the fatigue life and can therefore be considered an abstract figure. Although DFF values are relatable to daily practice, they do not bear a relation with the uncertainty in fatigue damage accumulation. In daily practice, a DFF of four means that a damage of 0.25 is acceptable. This is commonly interpreted as a fatigue life of 100 years for a design life of 25 years, which sounds reassuring to operators and regulators. However, the validity of this interpretation is subject to uncertainties related to both the fatigue life and the stress level.

When adopting probabilistic instead of deterministic methods, an essential parameter is the uncertainty of the design parameters. These uncertainty ranges do not follow easily from a design process or accumulated experience. There is an increasing amount of interest in the scientific literature in defining uncertainties and reliability assessments of the fatigue life of ships and offshore structures. A detailed overview is given in [11,12]. A probabilistic approach to fatigue design of steel-welded structures is applied by [13–18], amongst others. Chryssanthopoulos [13] applies the (Basquin-type) S–N curve approach, using probabilistic formulations to improve the estimate of the probability and size of the initial crack for the fracture mechanics approach. The work of Márquez-Domínguez [14] is focused on fitting the DFFs of offshore wind turbines based on rough estimates of the uncertainty distributions. Márquez-Domínguez concludes that, in general, the DFFs should increase compared to the values in design standards to reflect the same reliability level as the design S–N curve excluding model uncertainties. Ambühl [15] presents a similar approach to the approach by Márquez-Domínguez [14] to study the reliability of wave energy converters. This is achieved using a variable local model uncertainty from [19] based on complexity of the determination of the SCF (based on finite element analysis or parametric equations). Velarde [16] presents a fatigue reliability analysis for a concrete offshore wind structure based on the mean S–N curve and uncertainties in the model input parameters (structural, soil, metocean, and fatigue damage). The result is expressed in terms of the reliability index β. Gao [17] applies the S–N curve scatter (as was conducted in [20]) and compares different damage accumulation models as alternatives to the linear damage accumulation model (LDAM) [8,9]. Zhao [18] focuses on offshore structures and calibrates the DFFs that are reported in DNV-ST-0126 [21]. The calibration procedure considers a single slope S–N curve formulation based on small-scale experimental data and the distributions of the uncertainties similar to the ones used in this paper. Zhao [18] concludes that the reported DFFs can be substantially lower than what is reported by DNV to achieve the intended annual probability of failure. This conclusion does not match with the findings by Márquez-Domínguez [14]. This difference is attributed to the use of a specific set of small-scale specimen data by Zhao [18] to obtain the applied S–N curves. Márquez-Domínguez [14] applies standard S–N curves.

Calibration of the DFFs as is performed by Márquez-Domínguez [14], Ambühl [15], and Zhao [18] enables a calibration on the horizontal axis (cycles) of the S–N curve. This method is easy to implement, but it does not reflect the uncertainties related to the stress range accurately. It ignores the model uncertainties on a global and local level, which affects the stress range that a structural detail experiences. In turn, the fatigue life is affected by the stress range to the power of 3 to 5. It is thereby argued that a proper calibration of the deterministic fatigue analysis should also incorporate a shift related to the stress range (vertical axis of the S–N curve). Secondly, whereas the tailored DFFs from [14,18] can account for differences in acceptable consequences, it does not account for local differences in uncertainties. A tailored probabilistic input, specific to a zone in the ship, enables to further improve the calculation. The cited works [14,15,18] are all for offshore applications and not for ships, making the scope extension to ships a novelty of this paper.

The goal of this paper is to provide a practical framework to translate the probabilistic analysis of fatigue life to a deterministic one. Probabilistic parameters are associated with severity of consequence and are translated to a tailored fatigue (FAT) class for the deterministic approach. The proposal is based on the approach in DNV-CG-0129 [5] and DNV-RP-C203 [6]. It adopts distributions and parameters suggested in DNV-CG-0129 [5] (ship structures), DNV-RP-C203 [6] (offshore structures), and the Joint Committee on Structural Safety (JCSS) [22] (metallic structures). This framework enables ship owners, structural engineers, and ship designers to select a FAT class which adequately reflects the consequence of failure of the detail as well as the location-specific uncertainty distributions. The implementation in the engineering process requires limited effort as the method is closely related to current deterministic design practice. Furthermore, the relative importance of the considered sources of uncertainty in the probabilistic model is studied to determine priorities for further research on input uncertainties.

The current design practice typically comprises a deterministic approach with a lower-bound design level of the S–N curve of the applicable FAT class as indicated in [5]. In the novel approach, the FAT class is selected to reflect the required location-specific reliability level, without requiring a probabilistic analysis by the designer. Hence, a standard deterministic fatigue analysis is performed, where only the applicable FAT class is adjusted to the tailored FAT class to include the probabilistic information. In this way, the current design practice is adhered to; in addition, it provides the designer with the flexibility to select a probability of failure (PoF) level suited for the location.

This paper focuses on the determination of the influence of uncertainties in the loading, loading effects, and response, under the assumption of a deterministic input of the Weibull distribution of the loading amplitudes. All reported probabilities of failure are thereby conditional to the load input and assumed uncertainties. It is noted that the distributions from DNV [5,6] and JCSS [22] are generic and subject to uncertainty in itself [12]. The analysis is performed for the Hot Spot Structural Stress Concept (HSSSC) and follows the

DNV-CG-0129 [5] closed-form damage estimate for a two-slope S–N curve and a Weibull distributed load, based on the LDAM [8,9].

2. Materials and Methods

A probabilistic model is created to perform fatigue analysis from global loads to fatigue damage. To incorporate probabilistic information in a deterministic framework, the authors propose a method based on a probabilistic analysis to assess the risks related to failure of a welded detail within the structure. The acceptable PoF depends on the consequence of such a failure. A required FAT class is selected to achieve this required reliability, allowing for a deterministic calculation to complete the fatigue analyses. The proposed approach differs from the calibrated DFF [14,15,18] since it explicitly enables a selection of a PoF level corresponding to location-specific uncertainties and reliability demands, whereas the DFF is a linear safety factor that is applied to the fatigue life N. Next to that, the tailoring on the vertical axis (load) better reflects the relatively high load uncertainties that drive the design. A Monte Carlo analysis of the spectral fatigue approach is performed to determine the probabilistic predicted fatigue life. The probabilistic model, as shown in Figure 1, is based on the probabilistic approach in DNV-CG-0129 [5] and DNV-RP-C203 [6]. The light grey blocks in Figure 1 represent the calculation nodes that are also part of the current deterministic analysis. The dark grey blocks represent the uncertainties that affect the distribution of the resulting probabilistic fatigue life. The white blocks indicate FE models, which are not part of the probabilistic analysis. This analysis results in a probability density function (pdf) of the predicted fatigue life, conditional to the load input and assumed uncertainties; see the bottom-left of Figure 1. The pdf is used to derive the tailored FAT class that corresponds to a user-defined and location-specific reliability level.

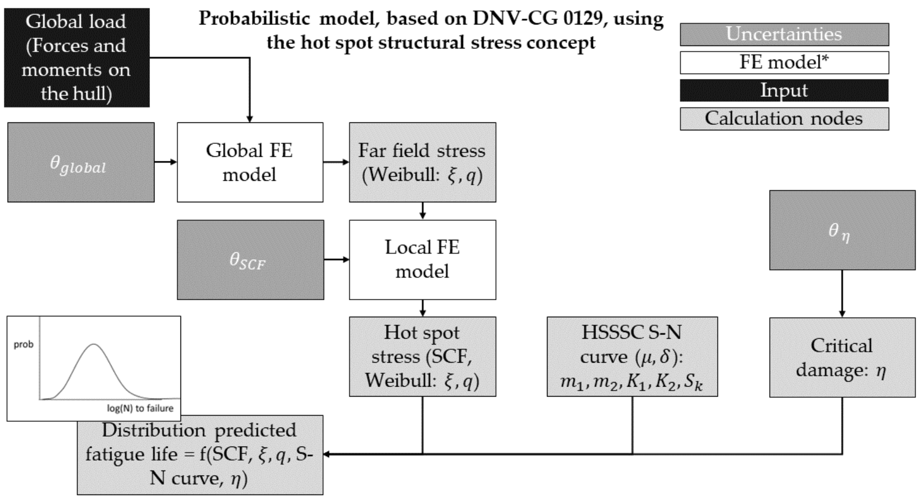

Figure 1. Diagram indicating the probabilistic model. * The white blocks indicate FE models that are not part of the probabilistic model.

In general, uncertainty can be separated into two categories: aleatoric uncertainty (being irreducible and objective, often used to describe intrinsic randomness of a phenomenon) and epistemic uncertainty (being reducible and subjective and is used to describe the uncertainties related to a, e.g., lack of knowledge, model simplifications, or incompleteness) [23]. The following uncertainties from DNV-CG-0129 and JCSS are taken into account:

- θ_{global}: global model uncertainty, accounting for uncertainties in both the wave-induced loading experienced by the ship and loading effects (DNV) or only the loading effects (JCSS). The aleatoric part covers the loading uncertainty (assuming that the operational area of the ship and the actual encountered wave conditions are

uncertain) and as-built geometry (e.g., plate thicknesses), whereas the epistemic part covers the translation to loading effects related to the global FE model of the structure.
- θ_{SCF}: local model uncertainty, accounting for the uncertainty in the determination of the Stress Concentration Factor (SCF). The aleatoric part covers the actual weld surface geometry, whereas the epistemic part covers model simplifications related to the HSSSC calculation method and the local FE model.
- θ_{η}: damage accumulation uncertainty, accounting for the simplifications made in the LDAM. This uncertainty is epistemic.
- δ: scatter in the S–N curve. This uncertainty is both aleatoric and epistemic. The aleatoric part covers the intrinsic variability in weld quality, weld surface geometry, welding processes, and material properties, whereas the epistemic part covers the S–N curve formulation (see, e.g., [24] for the scatter related to different fatigue strength concepts).

It is assumed that all sources of uncertainty are independent. This assumption is also made in the literature (e.g., [25]). The multiplication of θ_{global} and θ_{SCF} results in the combined uncertainty θ_{stress} which reflects the accumulated uncertainty related to the stress at the hot spot; see (1).

$$\theta_{stress} = \theta_{global}\theta_{SCF}, \tag{1}$$

The parameter θ_{stress} is multiplied with the scale parameter of the Weibull distribution that is assumed in the design (q_{design}) and the SCF to modify all considered stress levels accordingly; see (2). Any negative numbers that may result from the sampling of the distributions are corrected to their absolute value. Considering the scarcity of the occurrence of negative numbers, the influence of this correction on the outcome is considered negligible.

$$q = \theta_{stress} SCF q_{design}, \tag{2}$$

DNV-CG-0129 proposes a Weibull distribution for both the vertical wave bending moment (VWBM) and the stress range in the fatigue life prediction. The assumption of proportionality is used to apply the same Weibull shape parameter to the VWBM and stress range distribution. The Weibull shape parameter (ξ) remains deterministic, as is also assumed in DNV-RP-C210 [19]. The scatter in the S–N curve is explicitly accounted for by taking samples of the full S–N curve formulation with a standard deviation of $\delta = 0.2$ that effectively alters the location of the S–N curve knuckle. For each Monte Carlo sample, the intercepts $log_{10}(K_1)$ and $log_{10}(K_2)$ are calculated based on the modified location of the knuckle of the S–N curve. The slope remains unchanged in the calculation for both parts of the S–N curve. The probabilistic model is applied to an example case for a certain load range level and ship length. The Weibull shape parameter ξ is estimated from the VWBM for a rule length of 150 m. Only considering the VWBM is a simplification of the total load, which introduces uncertainty in itself; however, this simplification is applied here in line with other studies on the uncertainty of the fatigue loads [12]. For the VWBM, DNV [5] recommends the formulation of ξ [26] as given in (3):

$$\xi = 2.21 - 0.54 log_{10}(L), \tag{3}$$

in which L is the vessel rule length in m. For a rule length of 150 m, this yields $\xi = 1.035$. The stress range is assumed to be proportional to the VWBM. This assumption neglects any non-linearities in the loading and response, as well as the effect of pressure variations on the hull. For this example, the Weibull scale parameter q is selected for which the fatigue life with the currently applied deterministic approach from DNV-CG-0129 [5] is approximately 25 years; the value is thus $q_{design} = 13.7$ for the assumption of having 30% time at sea. This assumed that the time at sea, 30%, is based on a special purpose ship vessel that is considered within the project.

The two-parameter Weibull distribution is given by (4), in which S_i and n_i are the stress bins and number of cycles (normalized) at each stress bin level, respectively.

$$n_i = \left(\frac{\xi}{q}\right)\left(\frac{S_i}{q}\right)^{\xi-1} e^{-\left(\frac{S_i}{q}\right)^{\xi}} \tag{4}$$

The fatigue life N_i of each stress bin S_i is given by (5), based on [5]. m_1 and m_2 are the inverse slopes, and K_1 and K_2 are the intercepts of the S–N curve with the horizontal axis (N) on, respectively, the left and right side of the knuckle, located at S_k in MPa. FAT is the applied FAT class; in this example, it is FAT 90 due to the use of the HSSSC.

$$N_i = \begin{cases} \frac{K_1}{S_i^{m_1}} = \frac{10^{6.301+3\log_{10}(FAT)}}{S_i^{m_1}} \text{for } S_i \geq S_k \\ \frac{K_2}{S_i^{m_2}} = \frac{10^{7+5\log_{10}(0.585FAT)}}{S_i^{m_2}} \text{for } S_i < S_k \end{cases} \tag{5}$$

The results from (5) accumulate to a total life as given in (6).

$$N = \eta / \sum_{i=1}^{k} \frac{n_i}{N_i} \tag{6}$$

The probabilistic input of the model uncertainties (Table 1) is obtained from the design guidelines DNV-CG-0129 [5] and JCSS [22]. JCSS provides an estimate of the probabilistic input for each stochastic variable, whereas DNV [5] indicates a range. DNV-1 and DNV-2 give, respectively, the largest (and thereby conservative) and smallest variability of the indicated ranges in Table 1. DNV-3 is the reference distribution that is used in DNV-RP-C203 [6] to illustrate the mechanism of the DFF. This last set of distributions is only used to verify the model. The number of samples for the Monte Carlo analysis is set at 10^5. This sample size has been determined such that extra samples do not result in a different tailored FAT class when rounded to the nearest integer.

Table 1. Probabilistic input of the model uncertainties (mean, coefficient of variation).

Source	θ_{global}	θ_{SCF}	θ_{η}
DNV-1	N (1, 0.20)	N (1, 0.10)	LN (1, 0.30)
DNV-2	N (1, 0.15)	N (1, 0.05)	LN (1, 0.30)
DNV-3	combined: N (1, 0.25)		LN (1, 0.30)
JCSS	LN (1, 0.10)	LN (1, 0.20)	LN (1, 0.30)

The prediction of the fatigue life is based on the closed-form damage estimate from DNV-CG-0129 [5], based on a bi-linear S–N curve and Weibull distribution. The damage formulation is [5]:

$$D = N_D \left[\frac{q^{m_1}}{K_1} \Gamma\left(1 + \frac{m_1}{\xi}; \left(\frac{S_k}{q}\right)^{\xi}\right) + \frac{q^{m_2}}{K_2} \gamma\left(1 + \frac{m_2}{\xi}; \left(\frac{S_k}{q}\right)^{\xi}\right) \right] \tag{7}$$

in which D is the dimensionless fatigue damage, N_D is the design fatigue life in number of cycles, q is the Weibull scale parameter in MPa, ξ is the dimensionless Weibull shape parameter, and γ and Γ are the incomplete (lower) and complementary incomplete (upper) Gamma functions, respectively. The damage at the design fatigue life can be translated to the number of cycles at $D = \eta$ using:

$$N_{max} = \frac{\eta}{\left[\frac{q^{m_1}}{K_1} \Gamma\left(1 + \frac{m_1}{\xi}; \left(\frac{S_k}{q}\right)^{\xi}\right) + \frac{q^{m_2}}{K_2} \gamma\left(1 + \frac{m_2}{\xi}; \left(\frac{S_k}{q}\right)^{\xi}\right) \right]} \tag{8}$$

in which N_{max} is the predicted fatigue life and η is the critical damage in the LDAM.

2.1. Tailored FAT Class

For practical reasons and to promote the ease of implementation of the findings, the probabilistic model as described above is not recommended for engineering practice. Therefore, the probabilistic information is used to formulate a tailored FAT class. The applied initial FAT class for all structural details is a FAT 90. It is assumed that all tailored FAT classes, based on the original FAT 90, follow the bi-linear Basquin formulation and have an inverse slope of $m_1 = 3$ and $m_2 = 5$ on, respectively, the left and right side of the knuckle. This assumed Basquin-type formulation corresponds to the D curve in DNV-CG-0129 which is recommended for the HSSSC [5]. Figure 2 indicates the procedure to derive the tailored FAT class. The probabilistic model produces a pdf of the fatigue life as function of the model input; see Figure 3 for the histograms of the three considered probabilistic input sets for a sample size of 10^8. This pdf is presented in its cumulative form (cdf) enabling to read the fatigue life corresponding to a PoF level. The deterministic (currently applied) fatigue life prediction, based on the characteristic S–N curve with a FAT class and without accounting for any uncertainties (besides the S–N curve scatter), is performed with the FAT class as a variable. This function is optimized to obtain the same fatigue life and to determine the corresponding FAT class. This FAT class is now called the tailored FAT class because it reflects the probabilistic information that is tailored to the location of the structural detail.

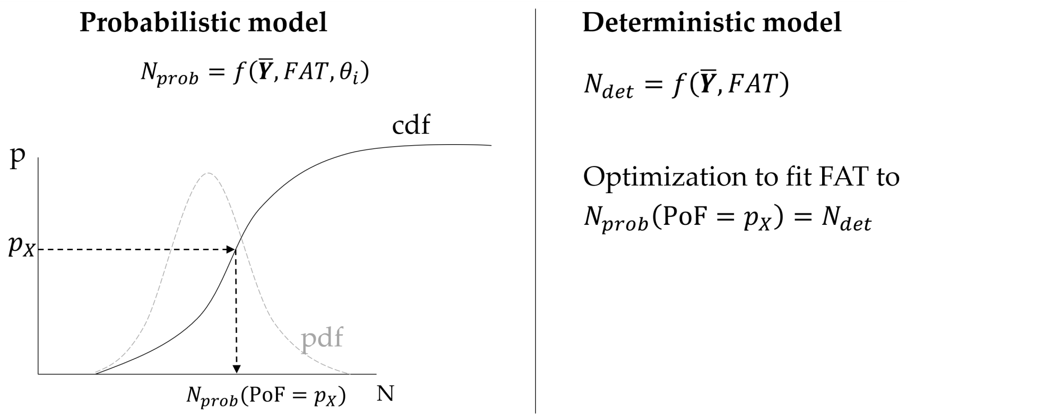

Figure 2. Diagram indicating the procedure to derive the tailored FAT class in which $\bar{\mathbf{Y}}$ is a vector containing the input parameters ξ and q, and p_X is the PoF level at which the tailored FAT is defined.

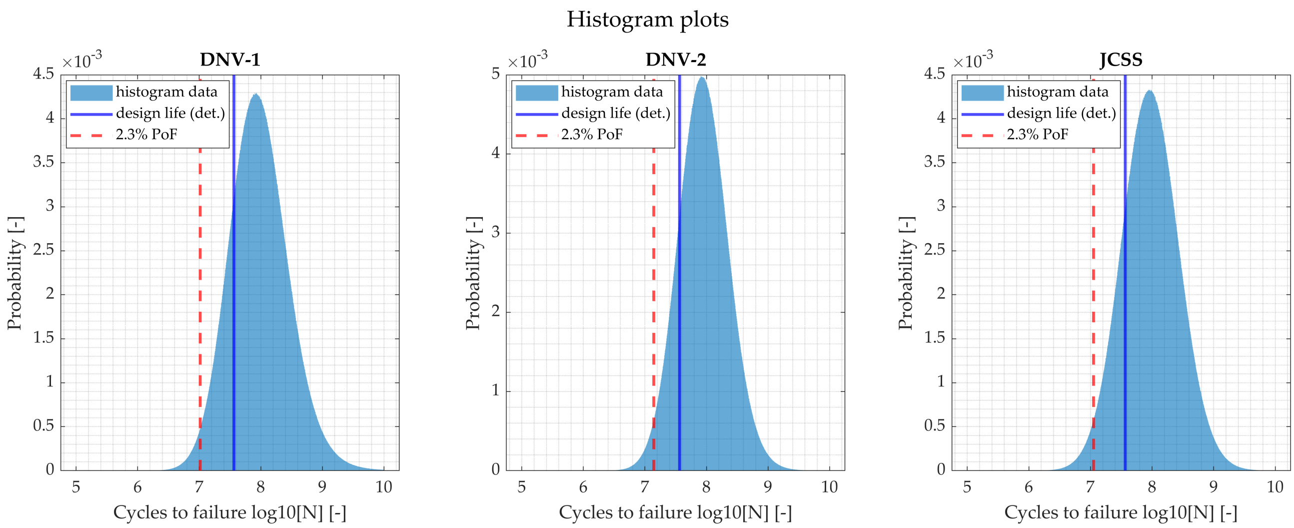

Figure 3. Histogram plots for the three different sets of uncertainty distributions based on 10^8 Monte Carlo samples, indicating the deterministic design life following from the DNV-CG-0129 calculation [5] and the 2.3% PoF from the histogram.

2.2. Sensitivity of the Probabilistic Parameters

The First Order Reliability Method (FORM) calculation is applied to identify the uncertainties with the largest relative importance in relation to the result of the fatigue life prediction. A FORM analysis calculates the weight (or sensitivity) factor α for each stochastic variable. The weight factors are a measure of the relative importance of the stochastic variables used in the limit state function to the probability of failure. The analysis applies linearization to the limit state function in the design point, which is the point where the limit state function equals zero with the highest probability density. Therefore, the design point gives the combination of loads and resistance where failure is most probable. The limit state function is expressed by

$$Z = \eta - D, \tag{9}$$

in which D is given by (7). It should be noted that the design fatigue life N_D is included in the analysis and is assumed to be 25 years. The influence of the assumed SCF, ship length (which affects the Weibull shape parameter), and Weibull scale parameter on the weight factors α is studied and reported in a variation study (Section 3.4).

3. Results

The results of the probabilistic model and resulting tailored FAT classes are presented for an example case with an SCF of 1.5, ship length L of 150 m, Weibull scale parameter q of 13.7 MPa, and adopting the HSSSC. The S–N curve scatter is accounted for in all performed analyses.

3.1. Tailored FAT Classes

The resulting tailored FAT classes of the example case are given in Table 2. Table 2 also indicates the PoF that corresponds to the fatigue life predicted with the deterministic approach (assuming no uncertainties apart from the reported scatter in the S–N curve). It is observed that this PoF is higher for the distribution sets with larger CoV values (DNV-1 vs. DNV-2). In the DNV documents, a design S–N curve is defined at 97.7% probability of survival [6]. The analysis of the deterministic analysis results in 2.3% PoF for a FAT 90, which matches the model as it corresponds with a 97.7% probability of survival [6]. A more detailed assessment of the differences between each case is included in the discussion.

Table 2. Tailored FAT classes rounded to the nearest integer at PoF levels for each of the reported sets of uncertainty distributions in combination with the example case (SCF of 1.5, ship length of 150 m, and $q_{design} = 13.7$ MPa) .

PoF	Reference *	DNV-1	DNV-2	JCSS
1%	86	65	71	63
2.5%	90	71	77	70
5%	94	77	82	77
10%	99	85	89	85
20%	105	95	97	95
PoF at FAT 90	2.3%	15.1%	11.3%	14.7%

* Indicating the FAT class in the conventional approach that accounts for the scatter in the S–N curve, but not for the uncertainties θ_{SCF}, θ_{global} and θ_{η} that are considered in this paper.

Table 2 shows that, for the same PoF, the tailored FAT classes based on the JCSS [22] distributions are lower than those based on the DNV distributions.

3.2. Comparison with the DFF

The maximum listed DFF in DNV-OS C101 [10] is three for "non-accessible areas, not planned to be accessible for inspection and repairs during operation". A higher DFF yields a higher level of conservatism and a lower predicted fatigue life. The results in this section are reported for DFFs equal to 1, 3, and 5 to reflect the range of DFF values in [10]; a case with DFF = 5 is included for illustration purposes. The number of samples for the Monte Carlo analysis is set at 10^8. This sample size has been determined such that extra samples do not result in a different obtained PoF value when rounded to one digit. The PoFs for each of the considered DFF values and each of the considered sets of uncertainty distributions are included in Table 3, which indicates a reduction of the conditional PoF for higher DFF values.

Table 3. Comparison of the PoF for the DFF value for each of the reported sets of uncertainty distributions.

DFF	Reference	DNV-1	DNV-2	JCSS
1	2.3%	15.1%	11.3%	14.7%
3	≤0.1%	0.9%	0.3%	1.1%
5	≤0.1%	0.1%	≤0.1%	0.2%

3.3. Verification

The model is verified based on the result of 2.3% PoF for a FAT 90 and DFF = 1 in Tables 2 and 3. A second verification is performed by comparing the findings to results in the literature. Both Lotsberg [27] and DNV-RP-C203 [6] report a graph that indicates the relation between the conditional PoF and the DFF. The data presented in both graphs are extracted and used for verification of the novel method presented in this paper. To extract a continuous formulation from the discrete data, a least-squares estimate cubic fit is applied to the data points in the graphs by Lotsberg and in DNV-RP-C203; see Figure 4. It should be noted that these fits are valid for DFFs in the range from 1 to 9.5, but not outside this domain.

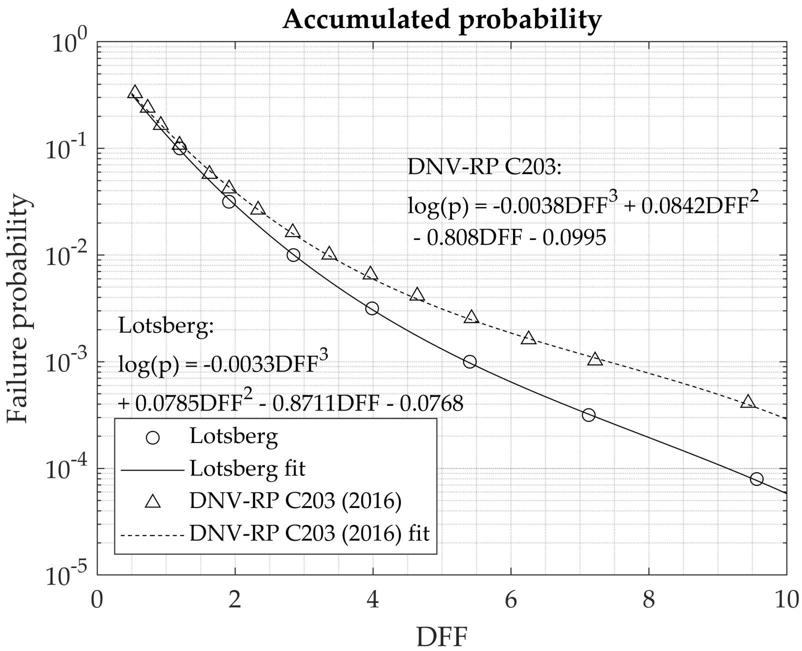

Figure 4. Least-squares cubic fits through the data on the relation between the DFF and failure probability from [6,27]. The markers correspond to the data points that are presented in the references [6,27] which are the input for the fit.

Next to the graph that indicates the relation between the DFF and PoF, Lotsberg [27] reports the PoF for three different DFF values for an example case of a single-sided butt weld between plates with a thickness of 25 mm. The results by Lotsberg [27] are obtained by an analytical approach whilst assuming a single-slope S–N curve. The studied detail is classified as F1, which corresponds to a FAT class of approximately FAT 63.

The comparison between the PoF at a DFF value for each of the models (analytical and FORM by Lotsberg [27], FORM from DNV-RP-C203 [6], and the present paper) is shown in Table 4. The Weibull shape parameter ξ is equal to 1. Next to that, for each studied variation, the CoV of θ_{stress}, the (bi-)linearity of the applied S–N curve, and the Weibull scale parameters for each DFF are reported in Table 4. Personal communication with Lotsberg [1] confirmed that for the FORM analysis, the CoV of the load is 20% instead of 25% as used in the analytical approach.

Table 4. Comparison of the PoF for DFF values as reported by Lotsberg [27], in DNV-RP-C203 [6], and obtained using the method as presented in this paper.

Data Source		Lotsberg [27]	Model in This Paper	DNV-RP-C203 [6]	Model in This Paper	Lotsberg [27]	Model in This Paper
CoV θ_{stress}		25%	25%	25%	25%	20%	20%
n slopes		1	1	2	2	2	2
Calculation method		analytical	Monte Carlo	FORM	Monte Carlo	FORM	Monte Carlo
DFF	**q (MPa)**	**PoF**	**PoF**	**PoF**	**PoF**	**PoF**	**PoF**
1	9.411	16.10%	15.2%	14.90%	18.1%	13.40%	15.0%
3	6.525	1.49%	0.8%	1.36%	2.3%	0.85%	1.2%
10	4.369	0.0263%	≤0.1%	≤0.1%	0.1%	≤0.1%	≤0.1%

It can be observed from Table 4 that the probability of failure of the model in this paper and as reported by Lotsberg [27] and in DNV-RP-C203 [6] are reasonably close together, but not identical. Comparing the FORM analysis and Monte Carlo simulations, the model in this paper results in higher PoF values. The observed differences in PoF in Table 4 could be attributed to numerical differences between the FORM-based approximation and the Monte Carlo method. Next to that, there is a numerical error related to the cubic fit through the digitized data in Figure 4. To conclude, this verification study shows that results are similar when comparing the model of this paper and the literature. Based on this, the conclusion is drawn that the model is successfully verified. This verification study also underlines the sensitivity of the probabilistic methods to the input as well as the selected calculation method and approximation.

3.4. Sensitivity Study Using FORM

The results of the FORM analysis are shown in Table 5. For the suggested parameters of DNV-1 and DNV-2 (see Table 1), it follows that the global model uncertainty θ_{global} and S–N curve scatter δ have the largest relative influence on the calculation fatigue life of the structure for the studied example case (SCF = 1.5, L = 150 m, $q_{design} = 13.7$ MPa). The assumed design life is 25 years with 30% time at sea.

Table 5. Weight factors of the example case, resulting from the FORM analysis.

Weight Factor	DNV-1	DNV-2	JCSS
α_{η}	0.35	0.41	0.33
$\alpha_{\theta_{global}}$	−0.66	−0.60	−0.36
$\alpha_{\theta_{SCF}}$	−0.37	−0.22	−0.71
α_{δ}	0.55	0.65	0.51

The results from Table 5 indicate that the weight factor of the global model uncertainty and S–N curve scatter are the largest for, respectively, the DNV-1 and DNV-2 distributions. For the JCSS distributions, the weight factor of the local model uncertainty is dominant. However, as was mentioned before, this difference can be attributed to differences in the definitions of global and local model uncertainties between DNV [5,6] and JCSS [22]. From Table 6, it can be concluded that for the DNV-1 distribution, the weight factors of $\alpha_{\theta_{global}}$ are the largest, followed by α_{δ}, for each of the variations. The absolute values of the weight factors changes slightly, but the conclusion of the relative importance does not. For future research, it is recommended to focus efforts on the refinement and/or reduction of the global model uncertainty, followed by the reduction of the scatter in the S–N curve.

Table 6. Weight factors resulting from the FORM analysis for variations in the case description, based on the DNV-1 distributions.

Case	SCF [-]	q_{design} [MPa]	L Ship [m]	α_{η} [-]	$\alpha_{\theta_{global}}$ [-]	$\alpha_{\theta_{SCF}}$ [-]	α_{δ} [-]
1—base case	1.5	13.7	150	0.35	−0.66	−0.37	0.55
2	1	13.7	150	0.37	−0.62	−0.38	0.58
3	2	13.7	150	0.33	−0.70	−0.36	0.53
4	1.5	6.9	100	0.38	−0.60	−0.39	0.59
5	1.5	6.9	200	0.38	−0.60	−0.38	0.59
6	1.5	27.4	100	0.30	−0.75	−0.34	0.48
7	1.5	27.4	200	0.29	−0.78	−0.32	0.46

4. Discussion

4.1. Obtained Tailored FAT Classes in Relation to Current Approach

It can be observed from Table 2 that the tailored FAT class, based on the probabilistic analysis and input applied in this paper, is lower than assumed in the deterministic approach. Next to that, the resulting tailored FAT classes are different for each set of uncertainty distributions in Table 1. For the global model uncertainty, the difference is attributed to a different scope of application of the uncertainty factor. For JCSS [22], the global model uncertainty only considers the loading effects [28]. Hence, it is related to the uncertainty in the engineering (e.g., finite element) model and does not cover the loading uncertainties. DNV [5,6] explicitly states that the global model uncertainty accounts for both the loading itself and the translation from load to load effects. This is in line with the larger reported CoV values for the DNV distributions [5,6] in Table 1. For the SCF uncertainty, it is possible that differences in the applied finite element analysis and industry-related best practices exist, possibly resulting in the variation in the assumed standard deviation for the SCF. This reduction of the FAT classes means that if the same PoF were to be obtained, the acceptable stress level for a structural detail must be reduced. This arguably makes the resulting design more conservative and might hinder implementation. This finding is in line with the conclusions from [14,15], which both conclude that the DFFs should in general be increased to reflect the same target reliability (excluding the effect of inspections). On the other hand, Zhao [18] concludes that re-calibrated DFFs can be lower than those used in design standards. However, the S–N curve that was applied is updated based on specific experimental data that deviate from the class S–N curves. The results from Zhao [18] can therefore not be compared 1-on-1 to the findings in this paper.

4.2. Benefits of Tailoring the FAT Class over Calibrating the DFF

Although a DFF can easily be visualized, a tailored FAT class is preferred for the following reasons, further elaborated below: (1) a calibration or tailoring procedure on the vertical (stress range) axis better reflects the large contribution of uncertainties related to the stress than a calibration on the fatigue life, and (2) reporting the probability of failure makes the non-linear nature of the relation between the DFF and probability of failure more insightful.

The approach of calibrating DFFs as performed in [14,15,18] does not consider the uncertainties on the vertical axis (stress range) of the S–N curve. However, tailoring the FAT class effectively poses a similar calibration but on a different axis. The results of the FORM analysis (Table 5) indicate that for the DNV-1 and DNV-2 distributions [5,6], the relative importances of η and θ_{SCF} are the lowest. The global model uncertainty θ_{global} and S–N curve standard deviation δ are, for these sets of input parameters, governing when using the prescribed calculation of DNV-CG-0129 [5]. The global model uncertainty might become more pronounced and governing when loading uncertainty and loading effects related to load and model simplification are accounted for separately and cumulatively. Next to that, the tail of the S–N curve is already uncertain due to a limited amount of available test data and the reduction of the fatigue limit as damage progresses. The confidence in the mid-cycle fatigue domain with loads above the initial fatigue limit is higher.

Lastly, a shift of the S–N curve based on the FAT class is deemed less confusing in communication. A DFF of two might wrongfully suggest a factor two increase of the fatigue life, whereas it merely reflects a factor two on the lower-bound design fatigue life, which can be observed from the non-linearity of the relation between the PoF and the DFF in Table 3. Lastly, the use of a DFF is not typically encountered for ship structures. The DNV-CG-0129 [5] specifically covers ship structures but does not mention the DFF in contrast to the documents that are applicable to offshore structures, e.g., [6,10].

4.3. Model Uncertainties and Tailored FAT Dependencies

The model of this paper is subject to epistemic uncertainty as a result of the following modeling choices:

- Application of a Basquin-type bi-linear S–N curve with a fixed slope on both sides of the knuckle point, following [5]. The slopes are m = 3 and m = 5 for stress ranges that are, respectively, higher and lower than that of the knuckle point.
- Application of the LDAM by [8,9], following [5], which ignores load sequence and load interaction effects.
- Simplifying the load to only consider the VWBM. Next to that, the stress level is assumed proportional to the VWBM. This assumption neglects any non-linearities in the loading and response, as well as the effect of pressure variations on the hull.
- Selection of a tailored FAT class that only poses a tailoring operation on the vertical axis of the S–N curve. The effects of the horizontal shift are implicitly (but not explicitly) incorporated through the optimization procedure.

The resulting reported tailored FAT classes can be applied under the assumption that the above modeling choices are valid for the application at hand. In case other effects are to be included, the model can be updated to incorporate more state-of-the-art fatigue modeling techniques.

For the dependencies of the reported tailored FAT classes to the case definition (SCF, Weibull scale parameter, and ship length), it can be concluded that the influence of the case definition on the tailored FAT classes is limited. The tailored FAT classes (rounded to the closest integer, based on 10^5 Monte Carlo samples) do not deviate more than 2 MPa over the variation cases 2, 3, 6, and 7 from Table 6. For variation case 4 and 5, the deviation is, respectively, 5 and 3 MPa.

4.4. Conditionality of the PoF

In the presented results, the PoF is conditional to the assumed distributions of the uncertainties related to the load level, global model, local model, and critical damage. Next to that, the probabilistic model is a model in itself, incorporating simplifications that can influence the results. The conditionality to the assumed load input does not deviate from the current deterministic approach. The conditionality to the assumed uncertainties is specific to the probabilistic approach. In reality, only the phenomenological parameters (hence excluding parameters strictly related to modeling) affect the scatter, which can be the actual variations in the modeling of the detail (θ_{SCF}), the scatter in the S–N curve (θ_{SN}), and the global loading effects (in part in θ_{global}). The actual PoF of a structural detail is likely to differ from the obtained conditional PoF, which is discussed in the section below. As was also stated in [14], the results are highly dependent on the assumed probabilistic input. Specification and refinement of this input might reduce this effect.

The present analysis is based on estimates from the literature of the distributions of the uncertainty factors. These are general factors that are not specific to a ship type and are thereby hypothesized to contain much variability. Adding to that, the widely used statistical parameters “often originate from outdated literature, limited experimental data, and assumptions” [12]. The global model uncertainty comprises both the loading uncertainty, which is considered in [29], and the transfer from global loads to far-field stresses at the detail of interest. The uncertainty in the transfer is affected by both the quality of the calculation and the production quality of the vessel. The level of detail in the numerical model influences the accuracy of the load paths, while the accuracy in terms of consistency between as-built and numerical model influences the actual stress levels. Lastly, the transfer function is chosen independent of loading condition, heading, and wave period. Including a transfer function that does take these variation into account will alter the results.

If the actual loading coincides with the currently assumed load input (based on the North Atlantic scatter diagram) and uncertainties, the actual PoF, when accounting for the model uncertainties, is higher than the intended 2.3% with the deterministic approach (PoF up to 15.1%; see Table 3). However, any deviations from the assumed operational profile due to, e.g., different operational areas, weather avoidance, actual heading, actual loading condition, and actual percentage of time at sea all may affect the actual PoF. To obtain 2.3% PoF, given that all other circumstances are equal, the effective time spent in, e.g., the North Atlantic has to be reduced. The influence of the time in seagoing operations can be studied with the assumption of an ergodic load distribution with the presented model. Next to that, changes in the operational area can be studied provided that representative time traces or load histograms can be obtained. It is recommended to study the influence of the scatter diagram (i.e., North Atlantic, World Wide Operation, or a specific dominant trade route) on the fatigue life prediction. This scatter diagram should be reflected in the formulation of the Weibull shape and scale parameter or in a realistic histogram to reflect the load.

The CoV of the SCF is in the same order of magnitude as that of the global model (see Table 1), depending on the chosen set of distributions. Round-robin results [30–32] indicate typical CoVs of the local model uncertainty in the order of 5%, making the global model uncertainty larger than the local model uncertainty. DNV-RP-C210 [19] indicates a recommended CoV of the distribution of local model uncertainty as a function of the complexity of the calculation method (e.g., FEA or (semi)analytical) of the SCF. It should be noted that this distribution in [19] does not account for any substantial deviations in weld quality compared to the S–N curve database; it merely accounts for variations in the local analysis.

The load interaction effect refers to the influence of the order of the variable amplitude loading on the accumulated fatigue damage. This phenomenon is not incorporated in the current model, although the literature suggests a relation between the spectrum type and shape and the critical damage [33–37]. The uncertainty related to the load interaction effect is reflected in the damage criterion. This uncertainty could be reduced when the LDAM [8,9] is replaced by a non-linear damage criterion that can account for load interaction effects such as the model from [38].

4.5. Implementation in Practice

The presented approach with tailored FAT classes enables a designer or customer to select the appropriate (conditional) PoF for a structural detail. This choice can be made based on the expected consequence and an acceptable risk level as well as on the uncertainties that are specific to the considered location. However, the uncertainties are not currently a variable input in the presented model; they could be included after more research is conducted.

To determine an adequate PoF for a welded detail, a so-called risk matrix [39] (Figure 5) can be adopted. The risk matrix indicates a risk as a function of the severity/consequence and the likelihood of occurrence. The resulting risk level is expressed in terms of expressions increasing from ‘minor risk’ to ‘severe risk’, from acceptable that ranges from as low as practically possible to unacceptable. This approach is getting more traction in the maritime industry to weigh the risk of alternative designs. No references were found that apply the approach of the risk matrix to the fatigue life prediction of ships. However, the JCSS [22] indicates a table with target reliability indices as a function of the consequence (minor–moderate–large) and cost of a safety measure (large–normal–small). In the design stage, we assume that the cost of the safety measure (i.e., redesign) is the same for all details and is therefore omitted in this present analysis.

5 x 5 RISK MATRIX						
PROBABILITY	Highly Probable	5 Moderate	10 Major	15 Major	20 Severe	25 Severe
	Probable	4 Moderate	8 Moderate	12 Major	16 Major	20 Severe
	Possible	3 Minor	6 Moderate	9 Moderate	12 Major	15 Major
	Unlikely	2 Minor	4 Moderate	6 Moderate	8 Moderate	10 Major
	Rare	1 Minor	2 Minor	3 Minor	4 Moderate	5 Moderate
		Very Low	Low	Medium	High	Very High
		IMPACT				

Figure 5. Outline of a typical risk matrix as used by IACS [39].

The risk matrix combines the severity with the likelihood. It is recommended to adopt one risk level for a ship (e.g., moderate). The severity level of a location in the ship structure can be based on a combination of the nature of the structural element (primary or secondary structure), accessibility for inspection, and the impact on downtime in case of failure. Thereafter, one can read out the maximum likelihood that corresponds to a certain severity level. This likelihood reflects the acceptable PoF. By way of illustration, one can select a butt weld in the bottom of the ship and a bracket toe connected to a longitudinal deck girder. A failure in the first location is unacceptable, as it comprises longitudinal strength and water-tightness, while the latter only gives a manageable effect on the longitudinal strength. To keep an equal risk for both details, this means that the required PoF is lower for the bottom detail than for the girder detail. The identification of the severity class can be linked to, e.g., water tightness (whether or not welded directly onto the shell plating [10]) and the influence of a failure on the structural integrity. It is recommended to define zones in the vessel that should have the same severity class to limit the efforts and potential for confusion and mix-ups in the design process.

Lastly, a paradigm shift is required to think in terms of actual probability of failure and move away from a 97.7% probability of exceedance of the S–N curve based on small-scale specimens (excluding all model uncertainties). This can be achieved in close cooperation with designers and structural engineers in the further development of the presented approach.

5. Conclusions

The goal of this paper is to provide a deterministic framework to translate the probabilistic analysis of fatigue life to tailored FAT classes at certain probabilities of failure. This paper has shown how a deterministic approach for fatigue analysis can be adapted to incorporate probabilistic information based on the DNV-CG-0129 [5] approach. A probabilistic model has been set up to find the conditional PoF based on the scatter in the S–N curve and the uncertainties in three main parameters: the global and local model uncertainties and the critical damage. With this model, tailored FAT classes can be calculated. These tailored FAT classes can be used in a deterministic approach to obtain the desired (conditional)

PoF for a specific structural detail. The selection of a tailored FAT class does not require the designer to alter the fatigue assessment approach; it merely changes one of the input parameters. Therefore, this method can easily be implemented in the design and analysis practice. The model has been verified with results from the literature.

The influence of the input parameters on the uncertainties is underlined by comparing different sets of uncertainties. Results show that tailored FAT classes are strongly dependent on the uncertainties. Distinct differences in the resulting tailored FAT classes have been found between input from the upper and lower bound of DNV [5,6], as well between DNV [5,6] and JCSS standards [22]. This emphasizes the need for careful consideration and specification of the uncertainties used. A FORM-based sensitivity study has shown that, for the DNV [5,6] distributions, the relative importance of the global model uncertainty and S–N curve scatter is governing over the local model uncertainty and LDAM uncertainty. This conclusion does not change for the studied variations on the base case. For the JCSS distributions (with a different definition of the global model uncertainty), the local model uncertainty and S–N curve scatter are governing. However, due to the more specific scope of the DNV documents [5,6], the findings for the JCSS distributions are not further considered here. The results of the FORM analysis thereby indicate that an efficient approach is to start with refinement and reduction of the global model uncertainty.

Based on a desired PoF, tailored FAT classes are obtained which are lower than the currently applied FAT classes. This means that the direct application of the findings in this paper would result in more conservative designs compared to the application of the deterministic approach, which in turn can hinder implementation in design practice. However, the currently presented tailored FAT classes are based on generic uncertainty distributions. Refinement of these input parameters to the ship structural applications should give more accurate tailored FAT classes.

Recommendations for further research are

- refine the probabilistic input (uncertainties) to enable input as a function of the location of the detail within the vessel, the building process specific to the ship type, ship yard, and operational profile.
- improve the probabilistic input, which can be combined with the above-listed refinement. The scopes of DNV CG-0129 [5] and DNV RP-C203 [6] are not the same, but the equally suggested uncertainties indicate room for improvement through scope refinement as well as increased substantiation of the CoV values.
- adopt alternatives for the S–N curve formulation and damage accumulation model that are expected to reflect the damage accumulation under variable amplitude loading conditions more accurately using, e.g., [38,40]. These alternatives are for ease of implementation preferably only adopted in the probabilistic model and not in the resulting tailored FAT-based deterministic approach.
- obtain realistic histograms from measurements to reflect the realistic distribution of the load and adopt a histogram-based load formulation instead of the Weibull spectrum. This should include the variable transfer functions accounting for, e.g., heading and loading conditions.
- update the uncertainty distributions from full-scale fatigue test results (e.g., [41–45]). These specimens should incorporate the redundancy in terms of parallel load paths, as well as the actual residual stress levels and distributions.

Author Contributions: Conceptualization, M.L.D., C.H.H.v.B. and M.H.; methodology, M.L.D. and C.H.H.v.B.; software, M.L.D. and C.H.H.v.B.; verification, M.L.D.; formal analysis, M.L.D. and C.H.H.v.B.; investigation, M.L.D. and C.H.H.v.B.; resources, M.H.; writing—original draft preparation, M.L.D.; writing—review and editing, C.H.H.v.B. and M.H.; visualization, M.L.D.; supervision, M.H.; project administration, M.H.; funding acquisition, M.H. All authors have read and agreed to the published version of the manuscript.

Funding: This research receives no external funding.

Institutional Review Board Statement: Not applicable.

Informed Consent Statement: Not applicable.

Data Availability Statement: Not applicable.

Conflicts of Interest: The authors declare no conflict of interest.

Abbreviations

The following abbreviations are used in this manuscript:

CoV	Coefficient of Variation
DFF	Design Fatigue Factor
FAT	Fatigue detail category
FEA	Finite Element Analysis
FORM	First Order Reliability Method
HSSSC	Hot Spot Structural Stress Concept
LDAM	Linear Damage Accumulation Model
PoF	Probability of failure
SCF	Stress Concentration Factor
VWBM	Vertical Wave Bending Moment

Note

[1] Private conversation about failure probability diagram: Book 'Fatigue Design of Marine Structures' [27] and DNV-RP-C203 [6], August 2023.

References

1. Deul, M.L.; van Battum, C.H.H.; Hoogeland, M.; van Bergen, J.W. Consequence and uncertainty-informed fatigue life prediction of ships. In *Advances in the Analysis and Design of Marine Structures*, 1st ed.; Ringsberg, J., Guedes Soares, C., Eds.; CRC Press: London, UK, 2023; chapter Fatigue, pp. 437–444. [CrossRef]
2. *BS 7608*; Guide to Fatigue Design and Assessment of Steel Products. The British Standards Institution: London, UK, 2015.
3. *BV 611-NI-2020-11*; Guidelines for Fatigue Assessment of Ships and Offshore Units. Bureau Veritas Marine and Offshore: Paris, France, 2020.
4. ABS. *Commentary on the Guide for the Fatigue Assessment of Offshore Structures*; Technical Report April 2003; American Bureau of Shipping (ABS): Spring, TX, USA, 2010.
5. *DNV-CG-0129*; Fatigue Assessment of Ship Structures. DNV AS: Høvik, Norway, 2021.
6. *DNV-RP-C203*; Fatigue Design of Offshore Steel Structures. DNV AS: Høvik, Norway, 2021.
7. Hobbacher, A.F. *Recommendations for Fatigue Design of Welded Joints and Components*, 2nd ed.; Springer International Publishing: Cham, Switzerland, 2016. [CrossRef]
8. Palmgren, A. Die lebensdauer von kugellagern. *Z. Des Ver. Dtsch. Ing.* **1924**, *68*, 339–341.
9. Miner, M.A. Cumulative Damage in Fatigue. *J. Appl. Mech. Trans. ASME* **1945**, *12*, A159–A164. [CrossRef]
10. *DNV-OS-C101*; Structural Design of Offshore Units. DNV AS: Høvik, Norway, 2023.
11. ISSC Committee III.2. Committee III.2 Fatigue and Fracture. In Proceedings of the 20th International Ship and Offshore Structures congress (ISSC 2018), Amsterdam, The Netherlands, 9–14 September 2018.
12. Dong, Y.; Garbatov, Y.; Guedes Soares, C. Review on uncertainties in fatigue loads and fatigue life of ships and offshore structures. *Ocean Eng.* **2022**, *264*, 112514. [CrossRef]
13. Chryssanthopoulos, M.K.; Righiniotis, T.D. Fatigue reliability of welded steel structures. *J. Constr. Steel Res.* **2006**, *62*, 1199–1209. [CrossRef]
14. Márquez-Domínguez, S.; Sørensen, J.D. Fatigue reliability and calibration of fatigue design factors for offshore wind turbines. *Energies* **2012**, *5*, 1816–1834. [CrossRef]
15. Ambühl, S.; Ferri, F.; Kofoed, J.P.; Sørensen, J.D. Fatigue reliability and calibration of fatigue design factors of wave energy converters. *Int. J. Mar. Energy* **2015**, *10*, 17–38. [CrossRef]
16. Velarde, J.; Kramhøf, C.; Mankar, A.; Sørensen, J. Uncertainty modeling and fatigue reliability assessment of offshore wind turbine concrete structures. *Int. J. Offshore Polar Eng.* **2019**, *29*, 165–174. [CrossRef]
17. Gao, H.; Zhang, X.; Yang, X.; Zheng, B. A Novel Probabilistic Fatigue Life Prediction Method for Welded Structures Based on gPC. *Math. Probl. Eng.* **2021**, *2021*, 5534643. [CrossRef]
18. Zhao, W. Calibration of design fatigue factors for offshore structures based on fatigue test database. *Int. J. Fatigue* **2021**, *145*, 106075. [CrossRef]
19. *DNV-RP-C210*; Probabilistic Methods for Planning of Inspection for Fatigue Cracks in Offshore Structures. DNV AS: Høvik, Norway, 2021.

20. Kepka, M.; Kepka, M. Deterministic and probabilistic fatigue life calculations of a damaged welded joint in the construction of the trolleybus rear axle. *Eng. Fail. Anal.* **2018**, *93*, 257–267. [CrossRef]
21. *DNV-ST-0126*; Support Structures for Wind Turbines. DNV AS: Høvik, Norway, 2021.
22. JCSS. 3.12 Fatigue Models for Metallic Structures. In *JCSS Probabilistic Model Code Part 3: Resistance Models*; JCSS Internet Publication, 2013; pp. 1–19. Available online: https://www.jcss-lc.org/publications/jcsspmc/JCSS-3-12-Fatigue.pdf (accessed on 22 August 2023).
23. Pelz, P.F.; Pfetsch, M.E.; Kersting, S.; Kohler, M.; Matei, A.; Melz, T.; Platz, R.; Schaeffner, M.; Ulbrich, S. Types of Uncertainty. In *Springer Tracts in Mechanical Engineering*; Pelz, P.F., Groche, P., Pfetsch, M.E., Schaeffner, M., Eds.; Springer International Publishing: Berlin/Heidelberg, Germany, 2021; pp. 25–42. [CrossRef]
24. Qin, Y.; den Besten, H.; Palkar, S.; Kaminski, M.L. Mid- and High-Cycle Fatigue of Welded Joints in Steel Marine Structures: Effective Notch Stress and Total Stress Concept Evaluations. *Int. J. Fatigue* **2021**, *142*, 105822. [CrossRef]
25. Nikolaidis, E.; Kaplan, P. Uncertainties in stress analysis on marine structures. *Int. Shipbuild. Prog.* **1992**, *39*, 19–53.
26. Hovem, L. *Loads and Load Combinations for Fatigue Calculations—Background for the Wave Load Section for the DNVC Classification Note: Fatigue Assessment of Ships*; DNVC Report No. 93-0314; Technical Report; DNV: Høvik, Norway, 1993.
27. Mussardo, G. *Fatigue Design of Marine Structures Book*; Cambridge University Press: New York, NY, USA 2019; Volume 53, pp. 1689–1699.
28. JRC. *Reliability Background of the Eurocodes (Under Development)*; Technical Report; Joint Research Center: Brussels, Belgium, 2023.
29. Hageman, R.; Drummen, I.; Thompson, I.; Stambaugh, K. Fleet Structural Integrity through Monitoring and Data Fusion. In Proceedings of the 15th International Symposium on Practical Design of Ships and Other Floating Structures, Dubrovnik, Croatia, 9–13 October 2022; Vladimir, N., Malenica, Š., Senjanović, I., Eds.; Faculty of Mechanical Engineering and Naval Architecture: Dubrovnik, Croatia, 2022.
30. Nussbaumer, A.; Grigoriou, V. Round Robin on local stress evaluation for fatigue by various FEM software. In Proceedings of the 69th International Institute for Welding (IIW) Annual Assembly and International Conference 2016, Melbourne, Australia, 10–15 July 2016.
31. Fricke, W.; Kahl, A. Comparison of different structural stress approaches for fatigue assessment of welded ship structures. *Mar. Struct.* **2005**, *18*, 473–488. [CrossRef]
32. Ogeman, V.; Mao, W.; Ringsberg, J.W. Uncertainty in stress concentration factor computation for ship fatigue design. In Proceedings of the International Conference on Offshore Mechanics and Arctic Engineering—OMAE, San Francisco, CA, USA, 8–13 June 2014. [CrossRef]
33. Gurney, T. *Cumulative Damage of Welded Joints*, 3rd ed.; Woodhead Publishing: Cambridge, UK, 2006; pp. 1–442. [CrossRef]
34. Agerskov, H.; Ibsø, J.B. Fatigue Life of Plate Elements with Welded Transverse Attachments Subjected to Stochastic Loading. In *Nordic Conference on Fatigue*; Blom, A., Ed.; EMAS Publishers: West Midlands, UK, 1993; pp. 41–60.
35. Agerskov, H. Fatigue in steel structures under random loading. *J. Constr. Steel Res.* **2000**, *53*, 283–305. [CrossRef]
36. Petersen, R.I.; Agerskov, H.; Martinez, L.L. *Fatigue Life of High-Strength Steel Offshore Tubular Joints*; Technical Report; Department of Structural Engineering and Materials, Technical University of Denmark: Lyngby, Denmark, 1996.
37. Johannesson, P.; Svensson, T.; De Maré, J. Fatigue life prediction based on variable amplitude tests-Methodology. *Int. J. Fatigue* **2005**, *27*, 954–965. [CrossRef]
38. Leonetti, D.; Maljaars, J.; Snijder, H.H. Probabilistic fatigue resistance model for steel welded details under variable amplitude loading—Inference and uncertainty estimation. *Int. J. Fatigue* **2020**, *135*, 105515. [CrossRef]
39. IACS. *No. 127 Rev.1 Nov 2021: A Guide to Risk Assessment in Ship Operations*; Technical Report; IACS: 2012.
40. Leonetti, D.; Maljaars, J.; Snijder, H.H. Fitting fatigue test data with a novel S-N curve using frequentist and Bayesian inference. *Int. J. Fatigue* **2017**, *105*, 128–143. [CrossRef]
41. Dijkstra, O.; Vredeveldt, A.; Janssen, G.; Ortmans, O. Fatigue testing of large scale details of a large size aluminium surface effect ship. In Proceedings of the Practical Design of Ships and Mobile Units, The Hague, The Netherlands, 20–25 September 1998; Oosterveld, M., Tan, S., Eds.; Elsevier: Amsterdam, The Netherlands, 1998; pp. 865–872. [CrossRef]
42. Fricke, W.; Kahl, A.; Paetzold, H. Fatigue assessment of root cracking of fillet welds subject to throat bending using the structural stress approach. *Weld. World* **2006**, *50*, 64–74. [CrossRef]
43. Fricke, W.; Paetzold, H. Full-scale fatigue tests of ship structures to validate the S-N approaches for fatigue strength assessment. *Mar. Struct.* **2010**, *23*, 115–130. [CrossRef]
44. Lillemäe, I.; Liinalampi, S.; Remes, H.; Itävuo, A.; Niemelä, A. Fatigue strength of thin laser-hybrid welded full-scale deck structure. *Int. J. Fatigue* **2017**, *95*, 282–292. [CrossRef]
45. Rautiainen, M.; Remes, H.; Niemelä, A.; Romanoff, J. Fatigue strength assessment of complex welded structures with severe force concentrations along a weld seam. *Int. J. Fatigue* **2023**, *167*, 107321. [CrossRef]

Disclaimer/Publisher's Note: The statements, opinions and data contained in all publications are solely those of the individual author(s) and contributor(s) and not of MDPI and/or the editor(s). MDPI and/or the editor(s) disclaim responsibility for any injury to people or property resulting from any ideas, methods, instructions or products referred to in the content.